frontiers | Frontiers in Energy Research

TYPE Original Research
PUBLISHED 06 April 2023
DOI 10.3389/fenrg.2023.1111186

OPEN ACCESS

EDITED BY
Guangcai Gong,
Hunan University, China

REVIEWED BY
Zeyu Li,
South China University of Technology, China
Ranendra Roy,
Independent researcher, Kolkata, India

*CORRESPONDENCE
Jianbo Li,
ljb_198504@163.com

SPECIALTY SECTION
This article was submitted to Sustainable Energy Systems, a section of the journal Frontiers in Energy Research

RECEIVED 29 November 2022
ACCEPTED 28 March 2023
PUBLISHED 06 April 2023

CITATION
Zheng W, Zhou H, Xiao Z, Sun D, Song C, Zhang X and Li J (2023), Evaluation and optimization of a novel cascade refrigeration system driven by waste heat. *Front. Energy Res.* 11:1111186. doi: 10.3389/fenrg.2023.1111186

Evaluation and optimization of a novel cascade refrigeration system driven by waste heat

Weibo Zheng[1,2], Hongbin Zhou[2], Zhiyong Xiao[2], Dong Sun[2], Changshan Song[2], Xiaohan Zhang[2] and Jianbo Li[3]*

[1]College of New Energy, China University of Petroleum (East China), Qingdao, China, [2]Technical Testing Center, Shengli Oilfield Branch of Sinopec, Dongying, China, [3]School of Mechanical and Electronic Engineering, Shandong University of Science and Technology, Qingdao, China

Direct discharge of waste heat from internal combustion engines (ICEs) is unfavorable for the efficient and clean fuel utilization. Here, a novel combined absorption-compression cascade refrigeration cycle is proposed to efficiently capture low-grade waste heat and supply cooling capacity for food freezing in vessels or refrigerated trucks. The intention of this work lies in: i) Comprehensively evaluating the performances of the proposed system; ii) Gaining the optimal operating conditions of the system. Aimed that, analysis models of energy, exergy, economy, and environment are set up to evaluate the sweeping performances. Further, multi-objective optimization is introduced to obtain the optimal operating parameters including evaporation and condensation temperature of the low-temperature stage, generation temperature and condensation temperature of the high-temperature stage, and cascade temperature differences. By applying multi-objective optimization, the coefficient of performance and exergy efficiency of the system are elevated from 1.283 to 1.547, and 0.222 to 0.246, respectively, the discharge amount of carbon dioxide are reduced from 71.40 to 59.57 tons year^{-1}, and annual total cost are decreased from 16,028 to 15,055 $ year^{-1} compared to initial operating conditions.

KEYWORDS

waste heat recovery (thermodynamic analysis), cascade refrigeration, absorption, comprehensive evaluation, multi-objective optimization

1 Introduction

Waste heat exhausted from internal combustion engines occupy about 55%–65% of the released heat of fuel combustion, mainly taken away by engine coolant and exhaust gases and finally discharged to the atmosphere. Utilizing the waste heat to drive absorption refrigerator is an attractive research. The cascade refrigeration can widen temperature zone while ensuring its performance and is usually used on freezing occasions (Messineo, 2012). Among, absorption compression cascade refrigeration performs well due to its waste heat utilization. Many researchers have implemented amounts of studies on its performance evaluation, economy, and optimization of different cascade cycles.

Lee et al. (Lee et al., 2006) conducted a thermodynamic analysis on a cascade refrigeration cycle using CO_2 and NH_3 as refrigerants and determined the appropriate condensation temperature for optimizing the maximum COP and the minimum exergy destruction. Dopazo et al. (Alberto Dopazo et al., 2009) studied a NH_3/CO_2 cascade refrigeration system for low-temperature cooling and obtained the optimal low-temperature condensation temperature by exergy analysis and energy optimization.

Bouaziz et al. (Bouaziz and Lounissi, 2015) analyzed the performance, efficiency, and exergy destruction of a novel two-stage absorption refrigeration system, and found that its performance was better than the conventional two-stage absorption refrigeration. Loonissi et al. (Lounissi and Bouaziz, 2017) analyzed an absorption/compression refrigeration cycle with the working fluids of R124-DMAC and found the refrigerator had the excellent operating conditions in the generating temperature range of 65°C–85°C. Gholamian et al. (Gholamian et al., 2018) proposed an advanced exergy analysis method to evaluate a cascade refrigeration cycle and provided references for system design, analysis, and evaluation of energy systems. Cimsit et al. (Cimsit, 2018) made a thermodynamic analysis on a double-effect absorption compression cascade refrigeration and suggested that the components with high exergy destruction rates should be paid more attentions. Agarwal et al. (Agarwal et al., 2020) investigated the influences of critical operating parameters of a triple-effect absorption cascade refrigeration on COP, exergy efficiency, exergy destruction rate, and exergy destruction ratio, and found that the system's refrigeration coefficient and exergy efficiency were higher than the single effect and double effect absorption-compression cascade refrigeration system. Faruque et al. (Faruque et al., 2022) detailed a thermodynamic analysis of a triple effect cascade refrigeration system in ultra-low temperature application, and found that the highest COP and exergy efficiency was 0.5931% and 54.5% respectively when evaporating temperature was −100°C. Chi et al. (Chi et al., 2022) proposed a NH_3/CO_2 cascade refrigeration system with an ejector. They found that the COP and exergy efficiency of the system was about 5.4% and 4.8% higher than the conventional cascade refrigeration system.

How to evaluate a refrigeration system thoroughly? If only the thermodynamics criterion is considered, the system may be ideal but not friendly economically. If only the economic criterion is considered, the economic performance may be deficient. It may consume abundant energy or discharges amounts of pollutants to the environment. Therefore, a comprehensive evaluation criterion should be considered simultaneously, including thermodynamics, economic cost, and environmental influences. Aminyavari et al. (Aminyavari et al., 2014) modeled and analyzed an NH_3/CO_2 cascade refrigeration system from the perspectives of recycling, economy, and environment and obtained optimal design parameters of the system by applying a multi-objective genetic algorithm. Mosaffa et al. (Mosaffa et al., 2016) implemented economic and environmental analysis on an NH_3/CO_2 cascade refrigeration system with different flash tank intercoolers and obtained optimal operating conditions. Cui et al. (Cui et al., 2019) carried out energy, exergy, and economic analysis on a cascade absorption refrigeration for low-grade waste heat recovery and investigated the influence of various operating parameters on the thermodynamic properties and financial cost. Golbaten et al. (Golbaten Mofrad et al., 2020) compared and optimized the performance of a cascade refrigeration cycle based on the analytical methods of energy, exergy, economy, and environment and found that the system performance could be significantly improved by applying waste heat recovery. Kumar et al. (Kumar Singh et al., 2020) compared and analyzed the energy, exergy efficiency, and economy in a cascade refrigeration system and obtained the optimal working pairs. Mofrad et al.

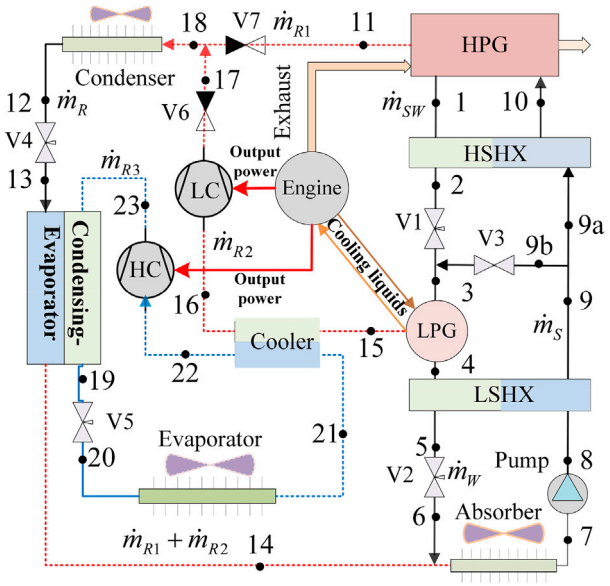

FIGURE 1
The combined absorption-compression cascade refrigeration system.

(Golbaten Mofrad et al., 2020) investigated a cascade refrigeration cycle with the heat recovery system. The optimization results revealed that applying the heat recovery cascade refrigeration cycle could increase 7.6% of COP and 12.5% of exergy efficiency. Yu et al. (Yu et al., 2020) analyzed a novel cascade absorption system driven by low-grade waste heat and optimized the system performance by implementing a multi-objective optimization method. Zhu et al. (Zhu et al., 2021) put forward a novel multi-target-temperature cascade system, and evaluated its optimum performances from the viewpoints of economics and thermodynamics and compared with other multi-temperature cascade systems. Mahmoudan et al. (Mahmoudan et al., 2021) evaluated a multi-level cascade system and conducted four different multi-objective optimization results. Hu et al. (Hu et al., 2022) analyzed a nested cascade refrigeration cycle with a heat recovery system and found it performed well in terms of energy, economy, and carbon emission. Gado et al. (Gado et al., 2022) assessed a cascade adsorption-compression refrigeration system by adopting renewable energy for cold storage applications based on power, exergy, exert economic, and environmental perspectives.

An absorption-compression combined refrigeration cycle activated by waste heat exhausted from an ICE to supply air-conditioning cooling capacity was proposed in our previous study (Jianbo et al., 2020). In another work, a novel cascade refrigeration with a compression refrigeration cycle cascaded in the process is proposed to provide low-temperature cooling capacity for food freezing in ships or refrigerated trucks (Han et al., 2021). Results showed that both cycles had excellent performance coefficients. However, the previous analysis is just based on thermodynamics and not comprehensive to assess its performances only from the view of thermodynamics. Here, a complete evaluation method is introduced to evaluate the

performance of the proposed cascade system. Firstly, assessing models including energy, exergy, economy, and environment (4E) are developed, and the evaluation results are analyzed under different operating conditions. Secondly, the multi-objective optimization is introduced to simultaneously gain the maximum efficiency and the minimum annual total cost. The work can guide the optimal design of the cascade system.

2 Modeling

2.1 Descriptions of the cascade refrigeration

As shown in Figure 1, the cascade refrigeration system (ACR) is composed of a high-temperature stage combined absorption-compression refrigeration cycle (AR) and a low-temperature stage CO_2 subcritical compression refrigeration cycle (CR). The working fluids of R124 and DMAC are used as refrigerant and absorbent in the AR, and R744 is used as the refrigerant of CR. The work principle is described as follows.

In the high-temperature stage cycle, the high concentration solution is heated by exhaust gases from an engine in the high-pressure generator (HPG). In the HPG, the heat of exhaust is transferred to the high concentration solution. Meanwhile, the vapor is generated and the solution becomes intermediate concentration solution. Then the solution is further heated by the engine's coolant in the low-pressure generator (LPG), and the solution becomes weak solution. The function of LPG is to effectively recover heat from the coolant of the internal combustion engine and produce some refrigerant vapor for low pressure compressor (LC). Refrigerant vapor from the LPG is cooled by the cooler to eliminate overheating and then is sucked and compressed by the low-pressure compressor (LC). The function of LC is to raise the pressure of the refrigerant vapor to the condensing pressure. The solution from the HPG participates in heat exchange in the high-temperature solution heat exchanger (HSHX), and the solution from the LPG participates in heat exchange in the low-temperature solution heat exchanger (LSHX). The functions of HSHX and LSHX are to enhance the heat utilization efficiency. Both the refrigerants generated in HPG and LHP enter the condenser, in which it is cooled to saturated or super-cooled liquid. After throttling, it enters the condensing evaporator, in which it is evaporated and supplies a low-temperature heat source for the CR cycle. Meanwhile, the low-temperature refrigerant is cooled to liquid in the condensing evaporator. Then, it enters the evaporator to produce a low-temperature cooling capacity. Finally, the vapor is sucked and compressed by the high-pressure compressor (HC).

2.2 Evaluation models

2.2.1 Energy model

Equilibrium equations of mass flow and the mass fraction are expressed as

$$\dot{m}_{\mathrm{S}}\left(1-X_{\mathrm{S}}\right)=\dot{m}_{\mathrm{SW}}\left(1-X_{\mathrm{SW}}\right) \tag{1}$$

$$\dot{m}_{\mathrm{W}}\left(1-X_{\mathrm{W}}\right)=\dot{m}_{\mathrm{SW}}\left(X_{\mathrm{SW}}\right) \tag{2}$$

The isentropic efficiency of the compressor is calculated by the following formula [3]

$$\eta_{\mathrm{s}}=1-\left(0.04\times r_{\mathrm{P}}\right) \tag{3}$$

The energy balance equation is

$$\sum Q=\sum W+\sum \dot{m}_{\mathrm{out}}h_{\mathrm{out}}-\sum \dot{m}_{\mathrm{in}}h_{\mathrm{in}} \tag{4}$$

Equations (1–4) are extended in Table 1 for all the system components.

Coefficient of performance

$$\mathrm{COP}=Q_{\mathrm{EC}}\Big/\left(W_{\mathrm{HC}}+W_{\mathrm{LC}}+W_{\mathrm{Pump}}\right) \tag{5}$$

2.2.2 Exergy model

By applying the first and second laws of thermodynamics, the steady-state form of the equilibrium equation of the control volume can be expressed.

$$\frac{d\dot{E}_{\mathrm{CV}}}{dt}=\sum_{j}\dot{E}_{\mathrm{j}}^{\mathrm{Q}}-\dot{E}^{\mathrm{W}}+\sum_{i}\dot{E}_{\mathrm{in}}-\sum_{e}\dot{E}_{\mathrm{out}}-\dot{E}_{\mathrm{D}}=0 \tag{6}$$

Exergy consists of four elements: physical, chemical, potential, and dynamic terms. In the absence of electromagnetic, electric, nuclear, and surface tension effects, it is assumed that variation of potential energy and kinetic energy can be neglected (Bejan et al., 1995)

$$\dot{E}=\dot{E}^{\mathrm{PH}}+\dot{E}^{\mathrm{CH}} \tag{7}$$

Chemical exergy consists of reaction exergy, diffusion exergy, and mixing exergy. There is no chemical reaction in the system, so the reaction exergy is discharged. No mass and momentum exchange between the working mediums in the system and the outside exist, so diffusion and mixing exergy are discharged. So the chemical exergy is ignored in the system. Therefore, only physics exergy is considered in this work. The following formula determines it.

$$\dot{E}^{\mathrm{PH}}=\dot{m}\left[\left(h-h_{0}\right)-T_{0}\left(s-s_{0}\right)\right] \tag{8}$$

If a working fluid is liquid, it can be defined as a function of temperature and heat capacity (Cengel and Boles, 2005)

$$s_{\mathrm{A}}-s_{\mathrm{B}}=C_{\mathrm{p}}\ln\frac{T_{\mathrm{A}}}{T_{\mathrm{B}}} \tag{9}$$

According to the exergy balance Equations (6–9), the exergy destruction formulas for all components are listed in Table 2.

$$q_{\mathrm{v}}=\frac{Q}{\rho_{\mathrm{a}}C_{\mathrm{pa}}\left(t_{\mathrm{a2}}-t_{\mathrm{a1}}\right)} \tag{10}$$

Where the expression of '$t_{a2}-t_{a1}$' is the temperature difference of outside air.

The input power of the fan motor is expressed as

$$W_{\mathrm{fan}}=\frac{q_{\mathrm{v}}\left(\Delta P'+\Delta P''\right)}{\eta_{\mathrm{fan}}} \tag{11}$$

The dynamic pressure and static pressure can be expressed as (Hesselgreaves, 2001)

TABLE 1 Energy equations of the cascade refrigeration system.

Components	Mass balance equations	Energy balance equations
HPG	$\dot{m}_1 = \dot{m}_{SW}, \dot{m}_{11} = \dot{m}_{R1}, \dot{m}_{10} = \dot{m}_S$	$Q_{HPG} = \dot{m}_{SW}h_1 + \dot{m}_{R1}h_{11} - \dot{m}_S h_{10}$
LPG	$\dot{m}_3 = \dot{m}_{SW}, \dot{m}_4 = \dot{m}_W, \dot{m}_{15} = \dot{m}_{R2}$	$Q_{LPG} = \dot{m}_W h_4 + \dot{m}_{R2}h_{15} - \dot{m}_{SW}h_3$
HSHX	$\dot{m}_1 = \dot{m}_{SW}, \dot{m}_2 = \dot{m}_{SW}$ $\dot{m}_9 = \dot{m}_S, \dot{m}_{10} = \dot{m}_S$	$Q_{HSHX} = \dot{m}_S(h_{10} - h_9) = \dot{m}_{SW}(h_1 - h_2)$
LSHX	$\dot{m}_4 = \dot{m}_W, \dot{m}_5 = \dot{m}_W$ $\dot{m}_8 = \dot{m}_S, \dot{m}_9 = \dot{m}_S$	$Q_{LSHX} = \dot{m}_W(h_4 - h_5) = \dot{m}_S(h_9 - h_8)$
EC	$\dot{m}_{20} = \dot{m}_{21} = \dot{m}_{R3}$	$Q_{EC} = \dot{m}_{R3}(h_{21} - h_{20})$
CC	$\dot{m}_{19} = \dot{m}_{23} = \dot{m}_{R3}$	$Q_{CC} = \dot{m}_{R3}(h_{23} - h_{19})$
CA	$\dot{m}_{12} = \dot{m}_{18} = \dot{m}_R = \dot{m}_{R1} + \dot{m}_{R2}$	$Q_{CA} = \dot{m}_{R1}h_{11} + \dot{m}_{R2}h_{17} - \dot{m}_R h_{12}$
EA	$\dot{m}_{13} = \dot{m}_{14} = \dot{m}_R = \dot{m}_{R1} + \dot{m}_{R2}$	$Q_{EA} = \dot{m}_R(h_{14} - h_{13})$
Abs	$\dot{m}_6 = \dot{m}_W, \dot{m}_7 = \dot{m}_S, \dot{m}_{14} = \dot{m}_R$	$Q_{Abs} = \dot{m}_W h_6 + \dot{m}_R h_{14} - \dot{m}_S h_7$
Cooler	$\dot{m}_{15} = \dot{m}_{16} = \dot{m}_{R2}, \dot{m}_{21} = \dot{m}_{11} = \dot{m}_{R3}$	$Q_{Cooler} = \dot{m}_{R2}(h_{16} - h_{15}) = \dot{m}_{R3}(h_{22} - h_{21})$
HC	$\dot{m}_{22} = \dot{m}_{23} = \dot{m}_{R3}$	$W_{HC} = \frac{\dot{m}_{R3}(h_{23} - h_{22})}{\eta_s \eta_m \eta_e}$
LC	$\dot{m}_{16} = \dot{m}_{17} = \dot{m}_{R2}$	$W_{LC} = \frac{\dot{m}_{R2}(h_{17} - h_{16})}{\eta_s \eta_m \eta_e}$
Pump	$\dot{m}_7 = \dot{m}_8 = \dot{m}_S$	$W_{Pump} = \dot{m}_S(P_G - P_{Abs})/\rho_S$

TABLE 2 Exergy destruction equations.

Components	Exergy destruction equations
HPG	$\dot{E}_{D,HPG} = \dot{E}_{10} - \dot{E}_1 - \dot{E}_{11} + \dot{E}_{Exhaust,HPG}$
LPG	$\dot{E}_{D,LPG} = \dot{E}_3 + \dot{E}_4 - \dot{E}_{15} + \dot{E}_{Coolant,LPG}$
HSHX	$\dot{E}_{D,HSHX} = \dot{E}_1 + \dot{E}_9 - \dot{E}_2 - \dot{E}_{10}$
LSHX	$\dot{E}_{D,LSHX} = \dot{E}_4 + \dot{E}_8 - \dot{E}_5 - \dot{E}_9$
EC	$\dot{E}_{D,EC+fan} = (1 - \frac{T_0}{T_{EC}})Q_{EC} + \dot{E}_{20} - \dot{E}_{21} + W_{fan,EC}$
CE	$\dot{E}_{D,cas} = \dot{E}_{13} + \dot{E}_{23} - \dot{E}_{14} - \dot{E}_{19}$
CA	$\dot{E}_{D,CA+fan} = \dot{E}_{18} - \dot{E}_{12} + W_{fan,CA}$
Abs	$\dot{E}_{D,Abs+fan} = \dot{E}_6 + \dot{E}_{14} - \dot{E}_7 + W_{fan,Abs}$
Cooler	$\dot{E}_{D,Cooler} = \dot{E}_{15} + \dot{E}_{21} - \dot{E}_{16} - \dot{E}_{22}$
HC	$\dot{E}_{D,HC} = \dot{E}_{23} - \dot{E}_{22} + W_{HC}$
LC	$\dot{E}_{D,LC} = \dot{E}_{17} - \dot{E}_{16} + W_{LC}$
Pump	$\dot{E}_{D,Pump} = \dot{E}_8 - \dot{E}_7 + W_{Pump}$

The air flow rate is.

$$\Delta P' = \frac{\rho_a w_y^2}{2} \tag{12}$$

$$\Delta P'' = 0.108 \frac{b}{d_e}\left(\rho_a w_y\right)^{1.7} \tag{13}$$

Entrance exergy into the system can be expressed as

$$\dot{E}_{in} = W_{HC} + W_{LC} + W_{Pump} + W_{fan,CA} + W_{fan,EC} + W_{fan,Abs} + \dot{E}_{Exhaust,HPG} + \dot{E}_{Coolant,HPG} \tag{14}$$

Exit exergy of the system can be expressed as

$$\dot{E}_{out} = Q_{EC}\left(1 - \frac{t_0}{t_{CL}}\right) \tag{15}$$

Therefore, the total exergy destruction can be expressed as (TJJTEMoTPA, 1985)

$$\dot{E}_{D,total} = \dot{E}_{in} - \dot{E}_{out} = \sum_k \dot{E}_{D,k} \tag{16}$$

The energy efficiency of the system can be determined as (TJJTEMoTPA, 1985)

$$\eta_{Ex} = \frac{\dot{E}_{out}}{\dot{E}_{in}} = 1 - \frac{\dot{E}_{D,total}}{\dot{E}_{in}} \tag{17}$$

2.2.3 Economy model

Aimed at exploring the influences of operation parameters on the economic performance of the cascade system, it is necessary to implement the economic analysis. The capital cost and operating cost are considered in the total cost. Besides, the environmental cost of carbon dioxide emissions is also included in the total cost. Therefore, the total cost of the cascade system ($\dot{C}_{total}$) includes the capital cost $\left(\sum_k \dot{Z}_k\right)$, operating cost ($\dot{C}_{op}$), and environmental cost of carbon dioxide emission ($\dot{C}_{env}$), which can be expressed as

$$\dot{C}_{total} = \sum_k \dot{Z}_k + \dot{C}_{op} + \dot{C}_{env} \tag{18}$$

2.2.3.1 Capital cost

The heat exchangers occupy the principal cost of the system. The heat transfer area (A) of all heat exchangers involved in the system can be calculated as follow.

TABLE 3 Overall heat transfer coefficient of the cascade refrigeration system.

Components	Overall heat transfer coefficient
HPG	$U = \frac{1}{(\frac{1}{\alpha_i}+r_i)\frac{d_o}{d_i}+\frac{d_o}{2\lambda}\ln(\frac{d_o}{d_i})+r_o+\frac{1}{\alpha_o}}$
LPG	
Abs	
HSHX	
LSHX	
EC	$U = \frac{1}{(\frac{1}{\alpha_i}+\gamma_i+\frac{\delta}{\lambda})\frac{F_{of}}{F_i}+(\frac{\delta_{Al}}{\lambda_{Al}}+\frac{1}{\xi\zeta_\tau\alpha_o})\frac{F_{of}}{F_\tau+\eta_f\cdot F_f}}$
CE	$U = \frac{1}{\frac{d_0}{\alpha_i d_i}+r_i\frac{d_0}{d_i}+\frac{bd_0}{\lambda d_i}+r_o+\frac{1}{\alpha_o}}$
Cooler	
CA	$U = \frac{1}{(\frac{1}{\alpha_i}+\gamma_i)\frac{F_{of}}{F_i}+\frac{\delta}{\lambda}\frac{F_{of}}{F_i}+(\gamma_{of}+\frac{1}{\alpha_o})\frac{1}{\eta_0}}$

TABLE 4 Capital costs of the cascade refrigeration system.

Components	Capital cost
HPG	$Z_{HPG} = 516.621A_{HPG} + 268.45$
LPG	$Z_{LPG} = 516.621A_{LPG} + 268.45$
HSHX	$Z_{HSHX} = 516.621A_{HSHX} + 268.45$
LSHX	$Z_{LSHX} = 516.621A_{LSHX} + 268.45$
EC	$Z_{EC} = 1397A_{EC}^{0.89} + 629.05W_{fan,EC}^{0.76}$
CE	$Z_{cas} = 2382.9A_{cas}^{0.68}$
CA	$Z_{CA} = 1397A_{CA}^{0.89} + 629.05W_{fan,CA}^{0.76}$
Abs	$Z_{Abs} = 516.621A_{Abs} + 268.45$
Cooler	$Z_{Cooler} = 516.621A_{Cooler} + 268.45$
HC	$Z_k = (\frac{573\dot{m}_{R3}}{0.8996-\eta_s})(\frac{P_{23}}{P_{22}})\ln(\frac{P_{23}}{P_{22}})$
LC	$Z_k = (\frac{573\dot{m}_{R2}}{0.8996-\eta_s})(\frac{P_{17}}{P_{16}})\ln(\frac{P_{17}}{P_{16}})$
Pump	$Z_{Pump} = 308.9W_{Pump}^{0.25}$

$$A = \frac{Q}{U \times \Delta t} \tag{19}$$

Among them, Δt are the temperature differences of working fluids. U is the overall heat transfer coefficient, which is mainly decided by heat transfer coefficients inside the tube ($\dot{\alpha}_i$) and heat transfer coefficient outside the tube ($\dot{\alpha}_o$).

$$\alpha_i = \frac{\lambda_i}{d_i} Nu = 0.023 \frac{\lambda_i}{d_i} Re^{0.8} Pr^{0.3} \tag{20}$$

$$\alpha_o = 0.52 \frac{\lambda_0}{d_0} {Re_f}^{0.5} {Pr_f}^{0.36} \left(Pr_f / Pr_w\right)^{0.25} \tag{21}$$

The overall heat transfer coefficient of all heat exchangers is listed in Table 3 (Cooper and JDJhet, 1983; Shah and Sekulic, 2002; Bejan and Kraus, 2003).

Compared with other main components of the system, the investment cost of valves, refrigerants, and connecting pipes can be ignored. The capital costs of heat exchangers are listed in Table 4.

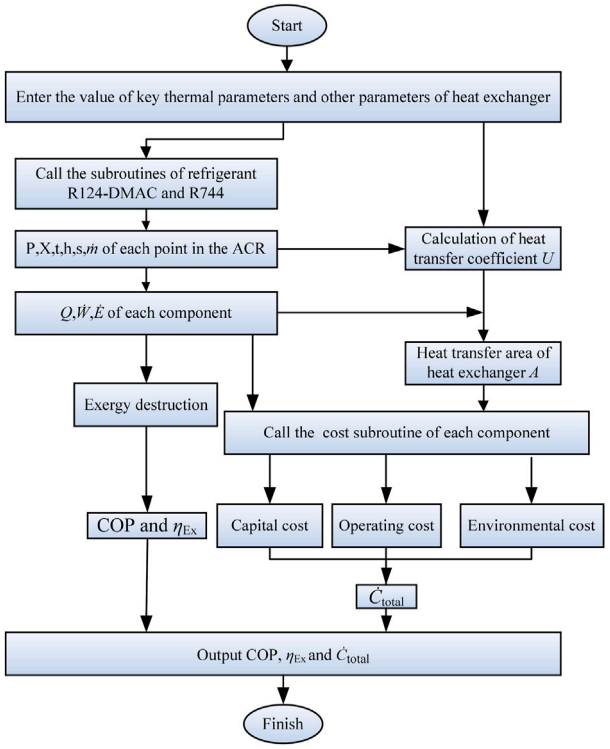

FIGURE 2
The simulation algorithm of combined absorption-compression cascade refrigeration system.

The corresponding cost is obtained by using the capital recovery factor (CRF) [34]

$$CRF = \frac{i(1+i)^N}{(1+i)^N - 1} \tag{22}$$

Where, CRF is a function of the annual interest rate (i) and N is the reference years (i.e., Service life).

Conversion of capital cost can be expressed as

$$\dot{Z}_k = CRF \times Z_k \times \phi \tag{23}$$

$$\forall k \in EQS \cap \{CA, EC, cas, HPG, HSHX, LPG, LSHX, Abs, Cooler, HC, LC, Pump\}$$

2.2.3.2 Operating cost

The operating cost includes the cost of the fuel and the electrical energy input of the compressor and solution pump, which can be expressed as

$$\dot{C}_{op} = top\left(\dot{C}_i^f \dot{B}_i + \dot{C}_i^{el} \dot{W}_i\right) \tag{24}$$

2.2.3.3 Environmental cost

Carbon dioxide emissions are considered to be an essential factor in the work, and the corresponding environmental cost can be expressed as

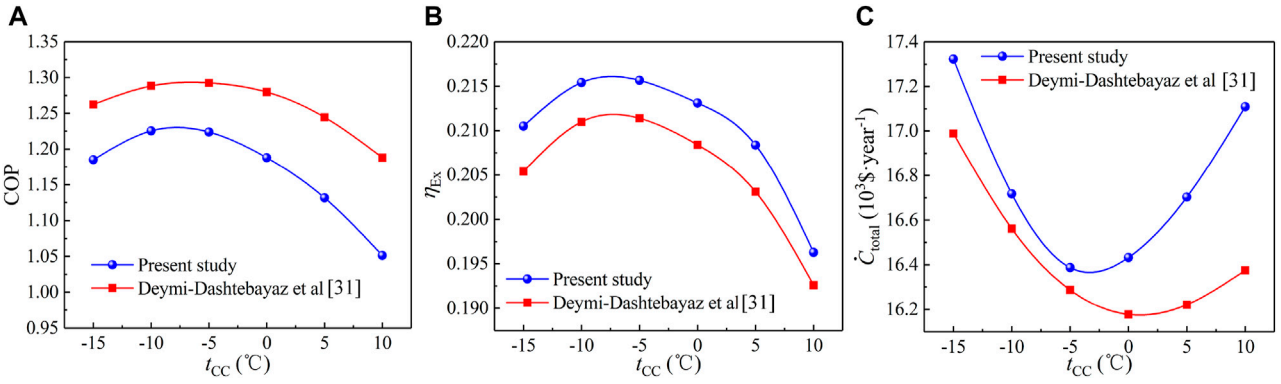

FIGURE 3
Comparison between modeling results in present study and computational results of Deymi [36]

$$\dot{C}_{env} = \frac{m_{CO_2}}{1000} \times \dot{C}_{CO_2} \quad (25)$$

Where, m_{CO_2} is obtained by the following formula

$$m_{CO_2} = \mu_{CO_2} W_t top \quad (26)$$

2.3 Simulation algorithm

Figure 2 shows the algorithm simulation model of the cascade refrigeration system. As shown in the figure, models of energy, exergy, and economy are all involved. The evaluation indexes, including COP, exergy efficiency (η_{Ex}), and annual total cost ($\dot{C}_{total}$) of the cascade refrigeration system, are taken into consideration in the model.

3 Results and discussions

3.1 Model verification

To validate the constructed models of the cascade refrigeration system, the basic performance parameters of the system, including the exergy destruction rate of all components, COP, the exergy efficiency, and annual total cost, are compared with the results by Deymi (Deymi-Dashtebayaz et al., 2021). The refrigerating capacity, ambient temperature, condensation temperature of the high-temperature stage, evaporation temperature of low-temperature phase and cascade temperature difference are 10 kW, 25°C, 40°C, −50°C, and 5°C, respectively.

As shown in Figure 3A, the variation trend of COP is similar, and the COP in this work is lower than that of Deymi under the same operating conditions. As shown in Figure 3B, the variation trend of exergy efficiency is similar, and the exergy efficiency of the cascade system is higher than that of Deymi. This is due to the fact that the waste heat of an internal combustion engine is rationally utilized in this work. As shown in Figure 3C, the annual total cost first declines and then increases with the rise of condensation temperature of the low-temperature stage. The total annual cost in this study is higher than that of Deymi due to more components in the proposed cycle. As shown, good agreements within an acceptable error between modeling results obtained for COP, the exergy efficiency, and annual total cost in this study and those presented by Deymi (Deymi-Dashtebayaz et al., 2021).

3.2 Comprehensive analysis and discussion

Based on the above models, the overall performances of the cascade cycle are analyzed and discussed by taking a combined absorption-compression cascade refrigeration system as a case using FORTRAN software. Essential parameters of the cascade system are listed in Table 5.

Grassmann diagram of exergy balance for the cascade refrigeration system is shown in Figure 4. As shown, the entrance exergy, the exit exergy, and the total exergy destruction are 21.353 kW, 4.605 kW, and 16.748 kW, respectively, when the refrigerating capacity, the ambient temperature, the condensation temperature of the high-temperature stage, the evaporation temperature of the low-temperature phase, cold refrigerated space temperature and cascade temperature difference are 15 kW, 25°C, 40°C, −50°C, −45°C, and 5°C, respectively.

The system's performance can be well observed by investigating the total exergy destruction of the proposed cycle. Under operating conditions of 15 kW refrigerating capacity and 45°Cof t_{Abs}, Variations of exergy destruction with operating temperatures are depicted in Figure 5.

Figure 5A shows that the exergy destruction of the cascade system declines with t_{EC} increasing from −55°C to −45°C. The power consumption of the fan and compressor decreases with the rise of t_{EC}, which means a reduction in input exergy. Therefore, a higher t_{EC} is beneficial for the reduction of total exergy destruction. As shown in Figure 5B, with *the* increase of t_{CC}, the total exergy destruction first decreases and then elevates, with a minimum value of 16.697 kW when t_{CC} is about −7.4°C. It can be concluded that an existing preferable t_{CC} is to minimize the total exergy destruction. It can be found in Figures 5C,D that the varying tendency of total exergy destruction elevates with the increase of t_{CA} and Δt_{cas}. The reason is that the rise of both t_{CA} and Δt_{cas} can cause a surge in

TABLE 5 Input values of the constant modeling parameters.

Parameter	Value (unit)
Cooling capacity	15 kW
Ambient temperature	25°C
Cold refrigerated space temperature	−45°C
Absorption temperature	45°C
Air density	1.1095 kg ·m^{-3}
Air constant pressure specific volume	1.013 kJ·(kg·K)$^{-1}$
Mechanical efficiency of compressor	0.93
Electrical efficiency of compressor	0.93
Annual interest rate	10%
Service life of equipment	15 years
Annual operation time	6,000 h
Maintenance cost factor	1.06 (Baghernejad, 2013)
Unit cost of electricity	0.06 $·kWh^{-1} (Aminyavari et al., 2014)
Unit cost of fuel	0.03785 $·kWh^{-1} (Rubio-Maya et al., 2012)
Carbon dioxide emission cost	90 $·ton^{-1} (Aminyavari et al., 2014)
Emission conversion factor of electricity	0.968 kg·kWh^{-1} (Aminyavari et al., 2014), (Wang et al., 2010)]

power consumption, which implies an increase of input exergy. Therefore, the lower t_{CA} and Δt_{cas} can promote the reduction of total exergy destruction.

Exergy efficiency (η_{Ex}) and coefficient of performance (COP) are crucial indexes in evaluating the cascade system. Usually, a high COP implies an excellent performance for a refrigeration system. However, the energy balance and conversion efficiency could not reflect the utilization degree of energy. So, it is necessary to analyze COP and η_{Ex} simultaneously. Figure 6 illustrates variations of COP and η_{Ex} with operating parameters.

As shown in Figure 6A, both COP and η_{Ex} increase with the rises of t_{EC} under the same working conditions. COP elevates from 1.085 to 1.374, with an increment of 0.289, and η_{Ex} also elevates from 0.20 to 0.23. The total power consumption declines with t_{EC} increasing, the input exergy decreases, and the output exergy remains unchanged. Both factors cause the increment of COP and η_{Ex}. Hence, a high t_{EC} is recommended from viewpoints of energy and exergy. As shown in Figure 6B, both COP and η_{Ex} first rises and then decline with the increase of t_{CC}. When t_{CC} is −7.4°C, COP reaches a maximum value of 1.231. When t_{CC} is −6.7°C, η_{Ex} has a maximum value of 0.216, which indicates that there is a preferable η_{Ex} to maximize the efficiency of the cascade system. As depicted in Figures 6C,D that both COP and η_{Ex} show downward tendencies with the rise of the t_{CA} and Δt_{cas}. The total power consumption of the system increases with the rise of the both temperatures, which causes the increase of input exergy and the decline of η_{Ex}. Therefore, the low t_{CA} and Δt_{cas} can enhance the performance of the system.

Based on the above analysis, the crucial parameters affecting the system are acquired based on the first and second laws of thermodynamics. Moreover, these parameters also affect the total cost. Therefore, the total cost of the cascade system, including capital cost, maintenance cost, and environmental cost of carbon dioxide emission also need investigation. Figure 7 shows the variation of annual total cost with the crucial parameters.

As shown in Figure 7A, annual total cost gradually declines with t_{EC} increasing from −50°C to −40°C. However the operating and environmental emission costs decline with the increase of t_{EC}. The decline of both is more obvious than the increase of capital cost. Therefore the annual total cost tends to gradual decline. As shown in Figure 7B, with t_{CC} increasing from −10°C to −2°C, annual total cost first decreases and then increases, and there is a minimum value of

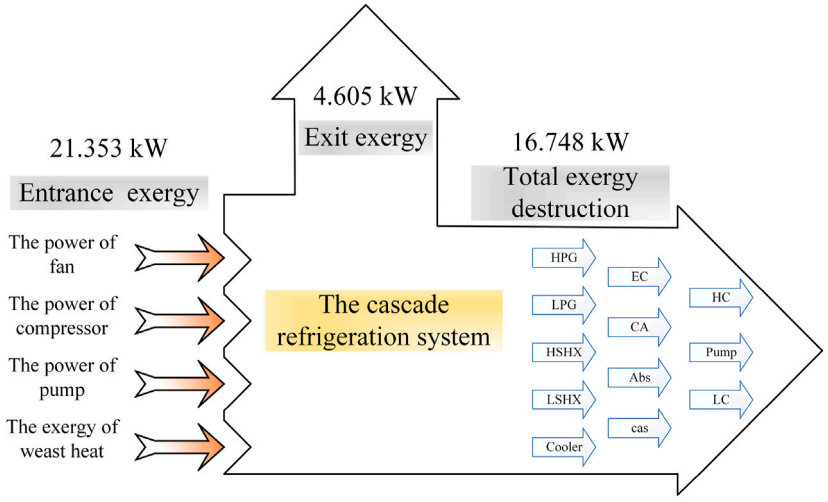

FIGURE 4
Grassmann diagram for exergy balance of the cascade refrigeration.

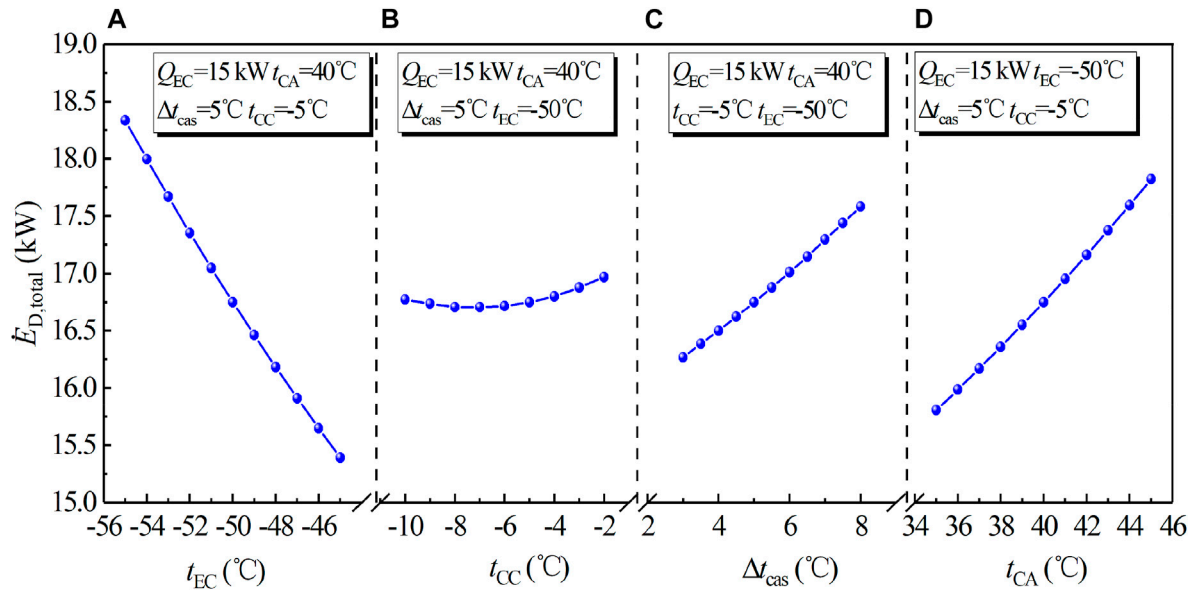

FIGURE 5
Variations of exergy destruction.

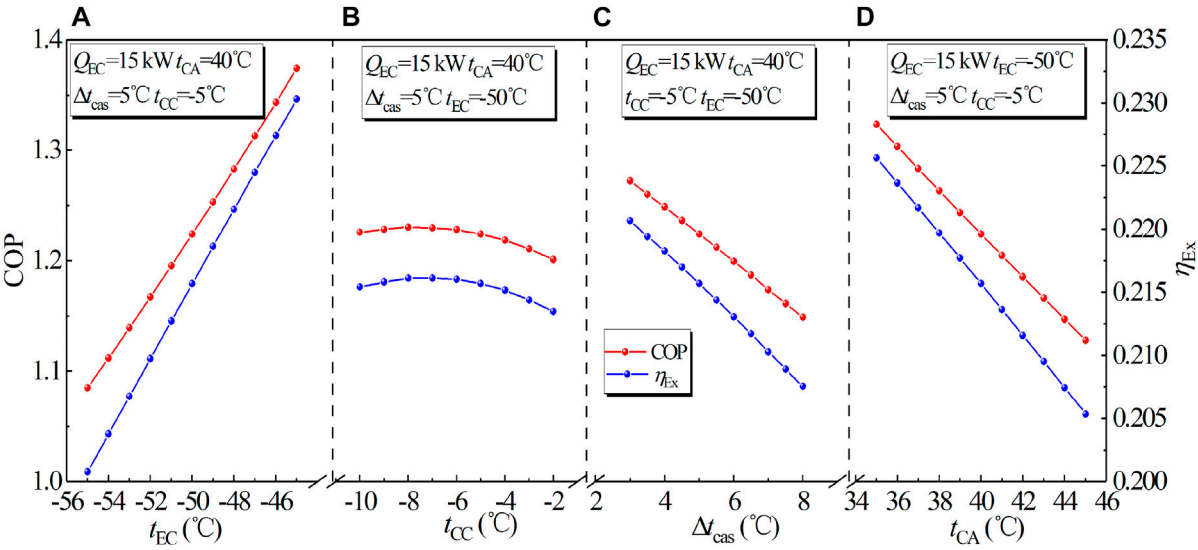

FIGURE 6
Variation of COP and exergy efficiency with CO_2 evaporation temperature and CO_2 condensation temperature, cascade temperature difference and R124 condensation temperature.

16,511.7 \$ year^{-1} when t_{CC} is −6.0°C. As shown in Figure 7C, with the increase of t_{CA} from 35°C to 45°C, the annual total cost first reduces and then increases with the rise of both temperatures, and there is a minimum value of 16,413.9 \$ year^{-1} when t_{CA} is 37.7°C. Under the same working conditions, Figure 7D shows the annual total cost elevates from 16,198.6 \$ year^{-1} to 17,290.6 \$ year^{-1}, with an increment of 1,092.0 \$ year^{-1}, when Δt_{cas} increases from 3°C to 8°C. It can be concluded that an appropriate reduction of Δt_{cas} is conducive to reduce the cost of the system.

The refrigeration system in this work is a combined absorption-compression cascade refrigeration system. High-pressure generator and low-pressure generator can ensure the most efficient use of the waste heat exhaust gases and jacket water from internal combustion engine of vehicles or ships and reduce energy consumption. Therefore, generating temperature plays a vital role on the performances in the cascade system.

Figure 8 shows the impact of the temperature of the high-pressure generator and low-pressure generator on the system thermo-economic

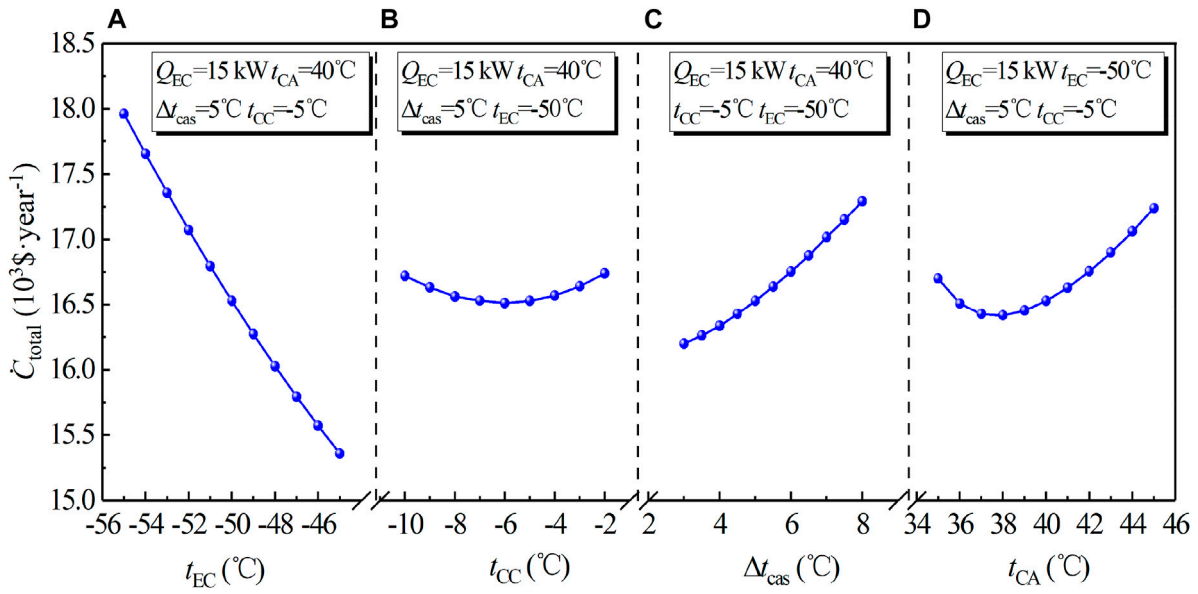

FIGURE 7
Variations of annual total cost under different thermal parameters.

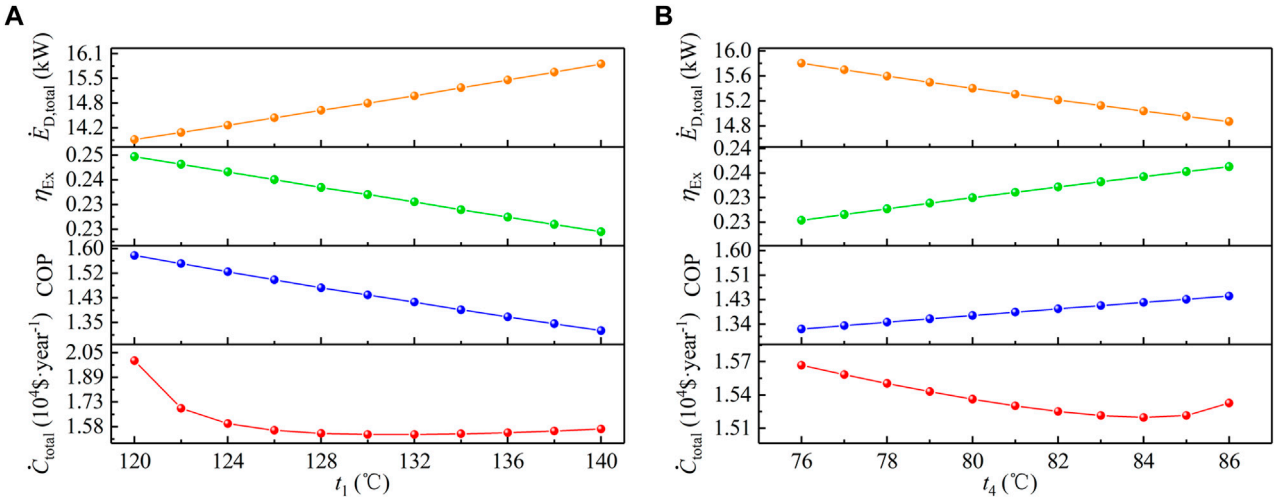

FIGURE 8
Variations of thermo-economic performances with generator temperatures.

performance under the same evaporator temperature, condenser temperature, cascade condenser temperature, absorber temperature and cascade condenser temperature differences. As shown in Figure 8A, the exergy destruction of the system rises, and exergy efficiency and performance coefficient are reduced with the temperature rise of high pressure generator (t_1). As t_1 increases from 120°C to 140°C, the annual total cost decreases rapidly at first, and then shows a trend of slow increase. The effect of the temperature of the low-pressure generator (t_4) on the cascade system thermo-economic performance is not quite the same as that of t_1. With t_4 rising from 76°C to 86°C (Figure 8B), the exergy destruction of the cascade system is elevated, while exergy efficiency and performance coefficient show the opposite trend. With the rise of t_4, the annual total cost declines first and then rises. There is a minimum annual total cost. When t_4 is 84°C, the annual total cost reaches a minimum value of 15,207.9 $ year^{-1}.

3.3 Multi-objective optimization

The optimal operating condition of the cascade system is worth studying to achieve the simultaneous optimization of performance index and economic index. Therefore the multi-objective optimization on the performance and economy for the cascade system is implemented in this section.

3.3.1 Optimization method and procedures

Three indexes including COP, η_{Ex}, and $\dot{C}_{total}$ are the primary evaluation indices for the system. COP and η_{Ex} are only related to operating temperatures, and $\dot{C}_{total}$ is related to working conditions and device scale. The high COP is the basis of a high-efficiency system when designing a refrigeration system. Under this case, the developed system may produce low exergy destruction. However, low exergy destruction usually implies a high investment cost. Therefore, the multi-objective optimization method is used to achieve good thermodynamics and economic performance simultaneously (Nasruddin et al., 2016). When η_{Ex} reaches the maximum, $\dot{C}_{total}$ should get the minimum. To express the optimization model more distinctly, the optimization method is implemented using the expression of $(1-\eta_{Ex})$ replacing η_{Ex}. The optimization model is transformed into minimization $(1-\eta_{Ex})$ and $\dot{C}_{total}$. The multi-objective optimization model can be expressed as follows

$$\min F(x) = [f_1(x), f_2(x)] \tag{27}$$

$$g(x) \le 0; y(x) = 0; x_l < x_u \tag{28}$$

Where $f_1(x)$ and $f_2(x)$ are the objective functions to be optimized (In this work, they represent $(1-\eta_{Ex})$ and $\dot{C}_{total}$ respectively), x is the decision variable to be iterated to find the optimal objective function, and $g(x)$ and $y(x)$ are the inequality and equality constraints of the optimization model, where x_l and x_u are the iterative limits of minimizing the input values (decision variables) of the objective function.

Four design variables affecting the performances of the system are considered, which is evaporation temperature (t_{EC}) and condensation temperature of the low-temperature stage (t_{CC}), condensation temperature of the high-temperature phase (t_{CA}), and heat transfer temperature difference (Δt_{cas}). According to the working conditions of the cycle, the range of each variable is restricted as follows

$$-56^{\circ}C \le t_{EC} \le -45^{\circ}C \tag{29}$$

$$-10^{\circ}C \le t_{CC} \le -2^{\circ}C \tag{30}$$

$$35^{\circ}C \le t_{CA} \le 45^{\circ}C \tag{31}$$

$$3^{\circ}C \le \Delta t_{cas} \le 10^{\circ}C \tag{32}$$

The objective function is calculated based on the genetic algorithm simulation model of multi-objective optimization. The specific calculation process is shown in Figure 9.

3.3.2 Optimization analysis

In this work, MATLAB software is used to solve the multi-objective optimization analysis model. Figure 10 shows correlations between the annual total cost ($\dot{C}_{total}$) and exergy efficiency (η_{Ex}) under the conditions of 15 kW refrigeration capacity and 45°C of t_{CA}. It can be found that $(1-\eta_{Ex})$ becomes smaller and the annual total cost declines with the rise of $\dot{C}_{total}$. It is difficult to meet the optimal thermodynamics performance and economy simultaneously. It also can be found that a higher η_{Ex} implies a higher $\dot{C}_{total}$. In this research, the vertical line of the Pareto optimal Frontier is chosen, and the intersection of the two is the best point of multi-objective optimization.

The linear weighted sum method is a Multi Criteria Decision Making (MCDM) technique, which assigns weight coefficients to each object according to its importance and then optimizes its linear combination to solve multi-objective programming problems. Linear weighted sum method has been employed for choosing the best optimum operating condition and parameter among the Pareto Front in this paper.

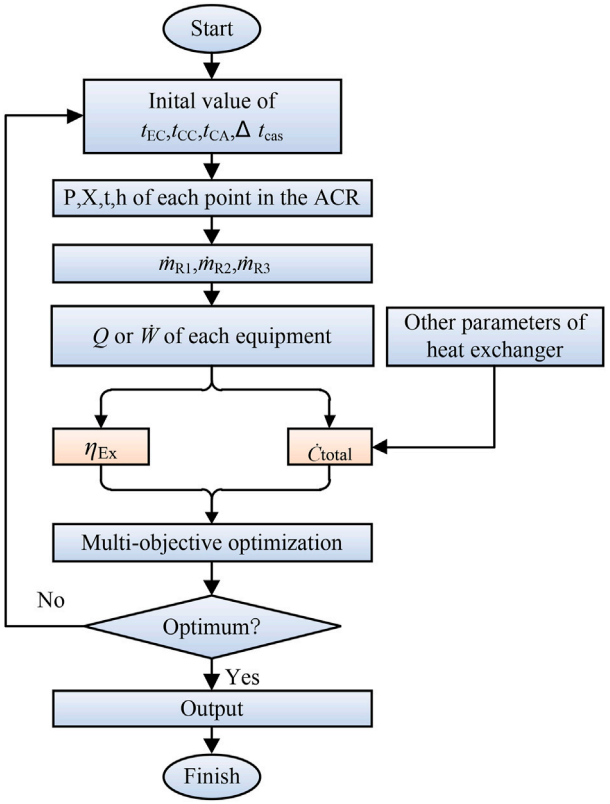

FIGURE 9
Schematic diagram of the multi-objective optimization.

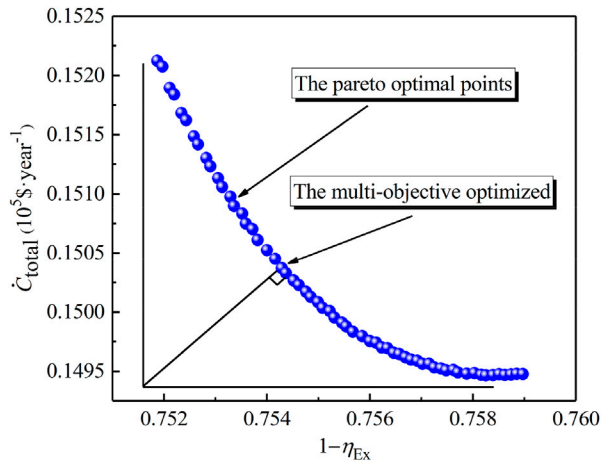

FIGURE 10
Pareto optimal Frontier from multi-objective optimization.

TABLE 6 Decision variables.

Decision variables	Base case	Thermodynamic optimization	Economic optimization	Multi-objective optimization
t_{EC} (°C)	−48.0	−45.0	−45.0	−45.0
t_{CC} (°C)	−5.0	−9.4	−7.0	−6.9
t_{CA} (°C)	40.0	35.0	37.7	35.9
Δt_{cas} (°C)	5.0	3.0	3.0	3.0

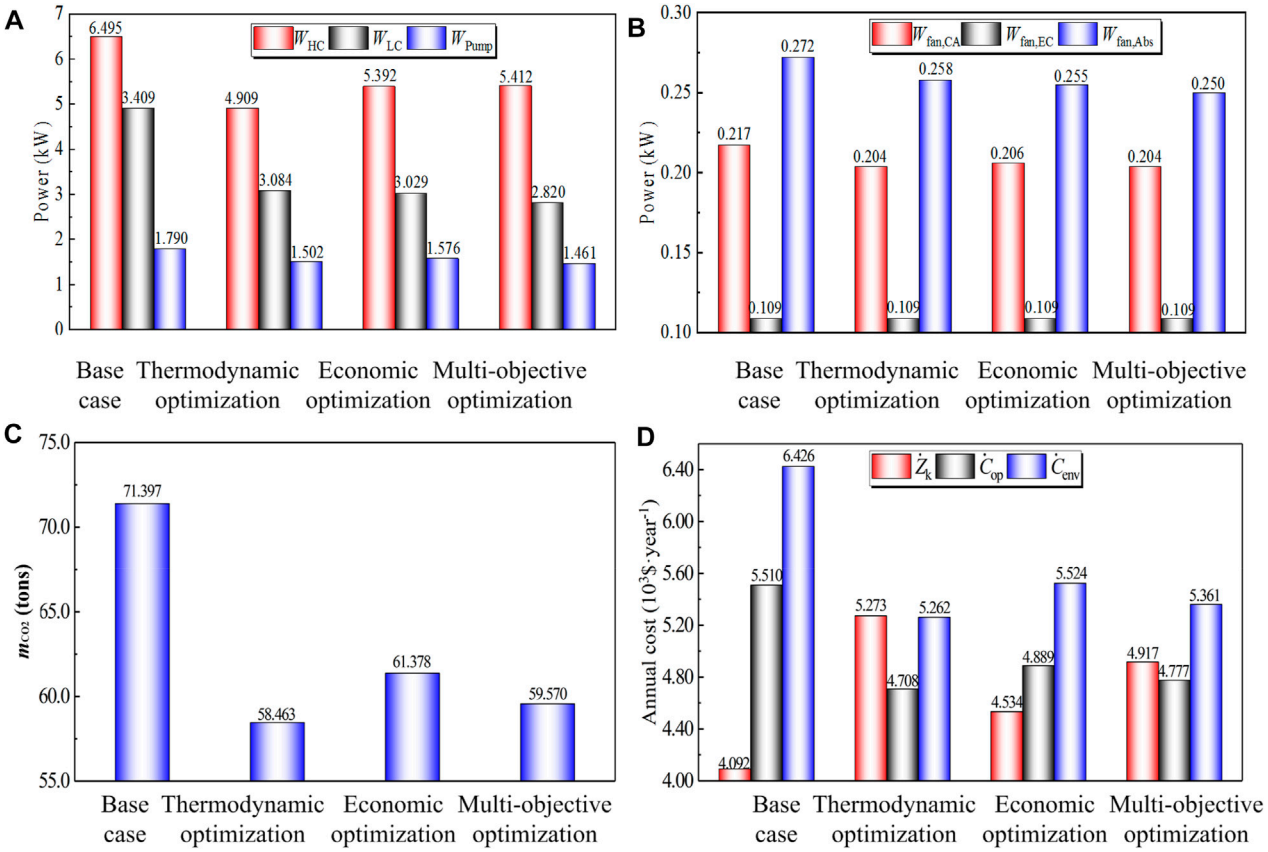

FIGURE 11
Comparison of power, CO_2 emissions and three kinds of annual costs.

Here are the steps of that MCDM.

For the Pareto Front data, the best optimum operating condition and parameter are selected and transformed into the optimal solution of the following functions.

$$\min_x \in \sum_{k=1}^{m} \omega_k f_k(x) \tag{33}$$

Where k = 2, m = 2, $f_1(x)$ is (1-η_{Ex}) and $f_2(x)$ is the annual total cost ($\dot{C}_{total}$), $\omega_k(x)$ is the weight coefficient.

$$\sum_{k=1}^{m} \omega_k = 1 \tag{34}$$

$\omega_1(x)$ is the weight coefficient of (1-η_{Ex}), and its value is 0.5, $\omega_2(x)$ is the weight coefficient of $\dot{C}_{total}$, 0.5.

The values of decision variables under different optimization mode are listed in Table 6. The power consumption, emission of CO_2, and three annual costs are shown in Figure 11 under the conditions of these decision variables in Table 6.

As shown in Figure 11A, the power of the pump and compressor are different for different optimization. HC has a minimum capacity of 4.91 kW when thermodynamic optimization is performed for the cascade system. Compared with the base case, the power of HC is reduced by 1.586 kW. When multi-objective optimization is performed, the power of LC and pump reach a minimum of 2.820 kW and 1.461 kW respectively, with respective decrements of 0.589 kW and 0.329 kW compared with the base case.

Figure 11B shows the power consumption of fans under different optimizations. These fans are used for heat

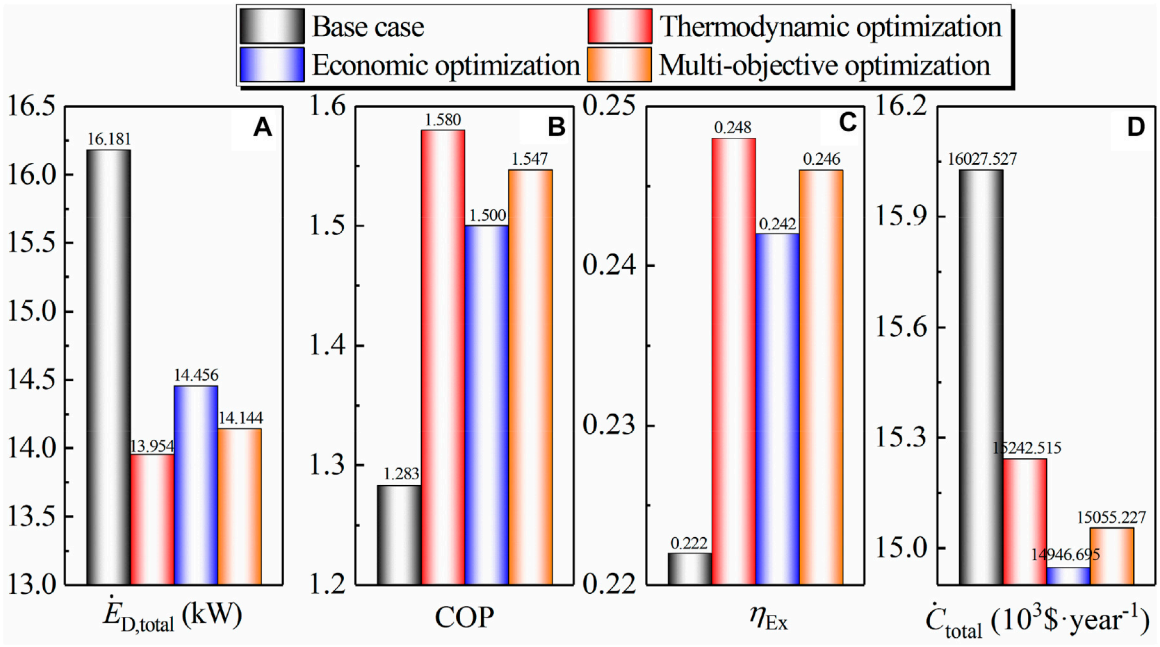

FIGURE 12
Comparison of Exergy destruction, COP, exergy efficiency and annual total cost.

dissipations of the condenser, the evaporator, and the absorber. The power consumption of evaporator fan for all the optimization methods is 0.109 kW. The minimum power consumption of the absorber fan is 0.250 kW in the multi-objective optimization, which is reduced by 0.022 kW compared with the base case. The emission of CO_2 strongly influences the environmental cost. As shown in Figure 11C, it can be found that the minimum emission of CO_2 under thermodynamic optimization is 58,462.7 kg, and it is 61,377.5 kg when the economics optimization is implemented. As shown in Figure 11D, the equipment cost reaches a minimum value of 4,534 \$ year^{-1} when economic optimization is implemented, and the operating cost reaches a minimum value of 4,708 \$ year^{-1} when thermodynamic optimization is implemented. Compared with the base case, the environmental cost is reduced from 6,426 \$ year^{-1} to 5,361 \$ year^{-1}, with a maximum reduction of 1,164 \$ year^{-1} when thermodynamic optimization is carried out.

It can be found in Figure 12A that the exergy destruction reaches a minimum of 13.954 kW under the condition of thermodynamic optimization and is reduced by 2.227 kW compared with the base case. It means that the performance improvement of system is also significant. The maximum exergy destruction under economic optimization conditions is 14.456 kW, decreasing to 14.144 kW under multi-objective optimization conditions. It can be found in Figures 12B,C that COP and exergy efficiency of the system can reach 1.580 and 0.248 respectively, based on thermodynamic optimization, the thermodynamic performance is the best at this time. Compared with the base case, COP and exergy efficiency are raised by 0.297 and 0.026 respectively, and the thermodynamic performance of the system was significantly improved. It can be found in Figure 12D that the lowest annual total cost is reduced from 16,027.5 to 14,946.7 \$ year^{-1} when the economy is optimized. As shown in Figures 12B,D, under the multi-objective optimization, the COP of the system can reach 1.547, the exergy efficiency can reach 0.246, and the annual total cost can drop to 15,055.2 \$ year^{-1}, balancing the thermodynamic and economic objectives. The combined cascade refrigeration system has the best operating conditions in this optimization case.

4 Conclusion

The overall performances of absorption-compression cascade refrigeration activated by the waste heat from ICE are evaluated from the viewpoints of energy, exergy, economy, and environment in this work. Firstly, the models of COP and exergy efficiency are obtained and validated by the previous study. Secondly, the exergy and economy analysis are implemented. Finally, the multi-objective optimization is introduced to acquire optimal operating parameters. Some conclusions can be drawn as follows.

1) Energy and exergy analysis indicate that the exergy destruction of the cascade refrigeration system has a minimum value of 16.697 kW when t_{CC} is about −7.4°C. Preferable COP of 1.231 and η_{Ex} of 0.216 can contribute to the high efficiency of the cascade system.
2) Economy and environmental analysis indicate that the annual total cost of the cascade system first declines and then rises with the increase of t_{CC} and t_{CA}. There is a minimum value of 16,511.7 \$ year^{-1} when t_{CC} is −6.0°C, and there is a minimum value of

16,413.9 \$ year^{-1} when t_{CA} is 37.7°C. By employing the multi-objective optimization, the COP, exergy efficiency and the annual total cost of the system can reach 1.547, 0.246, and 15,055.2 \$ year^{-1} respectively.

3) The thermodynamic and economic indexes under the multi-objective optimization are more excellent than that of the single-objective optimization.

Data availability statement

The original contributions presented in the study are included in the article/supplementary material, further inquiries can be directed to the corresponding author.

Author contributions

WZ: Conceptualization, Methodology, Software, Investigation, Formal Analysis, Writing—Original Draft; HZ: Data Curation, Writing—Original Draft; ZX: Visualization, Investigation; DS: Resources, Supervision; CS: Software, Validation XZ: Writing—Review and Editing JL (Corresponding Author):Funding Acquisition, Resources, Supervision, Writing—Review and Editing.

Funding

This research work is financially supported by the Natural Science Foundation of Shandong Province (No.ZR2020QE208), and National Natural Science Foundation of China (No. 52276205).

Conflict of interest

Authors WZ, HZ, ZX, DS, CS, and XZ were employed by the company Shengli Oilfield Branch of Sinopec.

The remaining author declares that the research was conducted in the absence of any commercial or financial relationships that could be construed as a potential conflict of interest.

Publisher's note

References

Agarwal, S., Arora, A., and Arora, B. B. (2020). Energy and exergy analysis of vapor compression–triple effect absorption cascade refrigeration system. *Eng. Sci. Technol. Int. J.* 23 (3), 625–641. doi:10.1016/j.jestch.2019.08.001

Alberto Dopazo, J., Fernández-Seara, J., Sieres, J., and Uhia, F. J. (2009). Theoretical analysis of a CO_2–NH_3 cascade refrigeration system for cooling applications at low temperatures. *Appl. Therm. Eng.* 29 (8-9), 1577–1583. doi:10.1016/j.applthermaleng.2008.07.006

Aminyavari, M., Najafi, B., Shirazi, A., and Rinaldi, F. (2014). Exergetic, economic and environmental (3E) analyses, and multi-objective optimization of a CO_2/NH_3 cascade refrigeration system. *Appl. Therm. Eng.* 65 (1-2), 42–50. doi:10.1016/j.applthermaleng.2013.12.075

Baghernejad, A., (2013). Thermoeconomic methodology for analysis and optimization of a hybrid solar thermal power plant. *Int. J. Green Energy* 10 (6), 588–609. doi:10.1080/15435075.2012.706672

Bejan, A., and Kraus, A. D. J. W. (2003). *Heat transfer handbook*. New Jersey, United States: John Wiley and Sons.

Bejan, A., Tsatsaronis, G., and Moran, M. J. (1995). *Thermal design and optimization*. New Jersey, United States: John Wiley and Sons.

Bouaziz, N., and Lounissi, D. (2015). Energy and exergy investigation of a novel double effect hybrid absorption refrigeration system for solar cooling. *Int. J. Hydrogen Energy* 40 (39), 13849–13856. doi:10.1016/j.ijhydene.2015.05.066

Cengel, Y. A., and Boles, M. A. (2005). *Thermodynamics: An engineering approach*. Europe: McGraw-Hill2009.

Chi, W., Yang, Q., Chen, X., Liu, G., Zhao, Y., and Li, L. (2022). Performance evaluation of NH_3/CO_2 cascade refrigeration system with ejector subcooling for low-temperature cycle. *Int. J. Refrig.* 136, 162–171. doi:10.1016/j.ijrefrig.2022.01.005

Cimsit, C. (2018). Thermodynamic performance analysis of the double effect absorption-vapour compression cascade refrigeration cycle. *J. Therm. Sci. Technol.* 13 (1), JTST0007–13. doi:10.1299/jtst.2018jtst0007

Cooper, A., and Jdjhet, U. (1983). *Heat exchanger design handbook*. Boca Raton: CRC Press.

Cui, P., Yu, M., Liu, Z., Zhu, Z., and Yang, S. (2019). Energy, exergy, and economic (3E) analyses and multi-objective optimization of a cascade absorption refrigeration system for low-grade waste heat recovery. *Energy Convers. Manag.* 184 (15), 249–261. doi:10.1016/j.enconman.2019.01.047

Deymi-Dashtebayaz, M., Sulin, A., Ryabova, T., Sankina, I., Farahnak, M., and Nazeri, R. (2021). Energy, exergoeconomic and environmental optimization of a cascade refrigeration system using different low GWP refrigerants. *J. Environ. Chem. Eng.* 9 (6), 106473. doi:10.1016/j.jece.2021.106473

Faruque, M. W., Nabil, M. H., Uddin, M. R., Monjurul Ehsan, M., and Salehin, S. (2022). Thermodynamic assessment of a triple cascade refrigeration system utilizing hydrocarbon refrigerants for ultra-low temperature applications. *Energy Convers. Manag.* 14, 100207. doi:10.1016/j.ecmx.2022.100207

Gado, M. G., Ookawara, S., Nada, S., and Hassan, H. (2022). Renewable energy-based cascade adsorption-compression refrigeration system: Energy, exergy, exergoeconomic and enviroeconomic perspectives. *Energy* 253, 124127. doi:10.1016/j.energy.2022.124127

Gebreslassie, B. H., Groll, E., and Garimella, S. V. (2012). Multi-objective optimization of sustainable single-effect water/Lithium Bromide absorption cycle. *Renew. Energy* 46, 100–110. doi:10.1016/j.renene.2012.03.023

Gebreslassie, B. H., Guillén-Gosálbez, G., Jiménez, L., and Boer, D. (2009). Design of environmentally conscious absorption cooling systems via multi-objective optimization and life cycle assessment. *Appl. Energy* 86 (9), 1712–1722. doi:10.1016/j.apenergy.2008.11.019

Gholamian, E., Hanafizadeh, P., and Ahmadi, P. (2018). Advanced exergy analysis of a carbon dioxide ammonia cascade refrigeration system. *Appl. Therm. Eng.* 137 (5), 689–699. doi:10.1016/j.applthermaleng.2018.03.055

Golbaten Mofrad, K., Zandi, S., Salehi, G., and Khoshgoftar Manesh, M. H. (2020). 4E analyses and multi-objective optimization of cascade refrigeration cycles with heat recovery system. *Therm. Sci. Eng. Prog.* 19, 100613–100627. doi:10.1016/j.tsep.2020.100613

Han, X., Li, J., Kong, X., Sun, T., Zhang, C., and Yin, L. (2021). Thermodynamic performance study on a novel absorption-compression cascade refrigeration activated by an internal combustion engine. *Int. J. Energy Res.* 45 (6), 9595–9612. doi:10.1002/er.6484

Hesselgreaves, J. E. J. M-H. B. C., Inc. Compact heat exchangers 2001.

Hu, R., Liu, X., Zhang, X., and Yang, L. (2022). Analysis of energy, economy, and carbon emission of nested cascade refrigeration cycle with heat recovery system. *Int. J. Refrig.* 136, 94–102. doi:10.1016/j.ijrefrig.2022.01.016

Jianbo, L., Kai, L., Xiaolong, H., Chen, Z., Fulin, C., and Xiangqiang, K. (2020). A novel absorption–compression combined refrigeration cycle activated by engine waste heat. *Energy Convers. Manag.* 205 (1), 112420. doi:10.1016/j.enconman.2019.112420

Kotas, T. J. (1985). *The exergy method of thermal plant analysis*. Amsterdam, Netherlands: Elsevier, 288–292.

Kumar Singh, K., Kumar, R., and Gupta, A. (2020). Comparative energy, exergy and economic analysis of a cascade refrigeration system incorporated with flash tank (HTC) and a flash intercooler with indirect subcooler (LTC) using natural refrigerant couples. *Sustain. Energy Technol. Assessments* 39, 100716–100733. doi:10.1016/j.seta.2020.100716

Lee, T-S., Liu, C-H., and Chen, T-W. (2006). Thermodynamic analysis of optimal condensing temperature of cascade-condenser in CO_2/NH_3 cascade refrigeration systems. *Int. J. Refrig.* 29 (7), 1100–1108. doi:10.1016/j.ijrefrig.2006.03.003

Lounissi, D., and Bouaziz, N. (2017). Exergetic analysis of an absorption/compression refrigeration unit based on R124/DMAC mixture for solar cooling. *Int. J. Hydrogen Energy* 42 (13), 8940–8947. doi:10.1016/j.ijhydene.2016.11.082

Mahmoudan, A., Samadof, P., Hosseinzadeh, S., and Garcia, D. A. (2021). A multigeneration cascade system using ground-source energy with cold recovery: 3E analyses and multi-objective optimization. *Energy* 223 (15), 121185–121202. doi:10.1016/j.energy.2021.121185

Messineo, A. (2012). R744-R717 cascade refrigeration system: Performance evaluation compared with a HFC two-stage system. *Energy Procedia* 14 (18), 56–65. doi:10.1016/j.egypro.2011.12.896

Mosaffa, A. H., Farshi, L. G., Infante Ferreira, C. A., and Rosen, M. (2016). Exergoeconomic and environmental analyses of CO_2/NH_3 cascade refrigeration systems equipped with different types of flash tank intercoolers. *Energy Convers. Manag.* 117 (1), 442–453. doi:10.1016/j.enconman.2016.03.053

Nasruddin, S. S., Giannetti, N., and Arnas, L. (2016). Optimization of a cascade refrigeration system using refrigerant C_3H_8 in high temperature circuits (HTC) and a mixture of C_2H_6/CO_2 in low temperature circuits (LTC). *Appl. Therm. Eng.* 104 (5), 96–103. doi:10.1016/j.applthermaleng.2016.05.059

Önder, K., Şencan, A., and Kalogirou, S. A. (2007). Thermoeconomic optimization of a LiBr absorption refrigeration system. *Chem. Engineering&Processing Process Intensif.* 46 (12), 1376–1384. doi:10.1016/j.cep.2006.11.007

Rezayan O, A. B., and Behbahaninia, A. (2011). Thermoeconomic optimization and exergy analysis of CO_2/NH_3 cascade refrigeration systems. *Energy Oxf.* 36 (2), 888–895. doi:10.1016/j.energy.2010.12.022

Rubio-Maya, C., Pacheco-Ibarra, J. J., Belman-Flores, J. M., Galvan-Gonzalez, S. R., and Mendoza-Covarrubias, C. (2012). NLP model of a $LiBr–H_2O$ absorption refrigeration system for the minimization of the annual operating cost. *Appl. Therm. Eng.* 37 (5), 10–18. doi:10.1016/j.applthermaleng.2011.12.035

Sayyaadi, H., and Nejatolahi, M. (2011). Multi-objective optimization of a cooling tower assisted vapor compression refrigeration system. *Int. J. Refrig.* 34 (1), 243–256. doi:10.1016/j.ijrefrig.2010.07.026

Shah, R. K., and Sekulic, D. P. (2002). *Fundamentals of heat exchanger design: Fundamentals of heat exchanger design*.

Tatchell, D. G. J. I. JoH., and Transfer, M. (1987). in *Handbook of single-phase convective heat transferSadik Kaka*. Editors R. K. Shah and W. Aung (New York: Wiley).

TjjtemoTPA, K. (1985). *The exergy method of thermal plant analysis*, 288–292.

Wang, J., Zhai, Z., Jing, Y., and Zhang, C. (2010). Particle swarm optimization for redundant building cooling heating and power system. *Appl. Energy* 87 (12), 3668–3679. doi:10.1016/j.apenergy.2010.06.021

Yu, M., Chen, Z., Yao, D., Zhao, F., Pan, X., Liu, X., et al. (2020). Energy, exergy, economy analysis and multi-objective optimization of a novel cascade absorption heat transformer driven by low-level waste heat. *Energy Convers. Manag.* 221 (1), 113162. doi:10.1016/j.enconman.2020.113162

Zhu, Y., Peng, Z., Wang, G., and Zhang, X. R. (2021). Thermodynamic analysis of a novel multi-target-temperature cascade cycle for refrigeration. *Energy Convers. Manag.* 243, 114380. doi:10.1016/j.enconman.2021.114380

Glossary

Nomenclature

b Fin width (m)
B Fuel exergy (kW)
$\dot{C}_{CO_2}$ Carbon dioxide emission cost ($·ton^{-1})
$\dot{C}_{el}$ Unit cost of electricity ($·kWh^{-1})
$\dot{C}_{env}$ Annual cost of environment ($·year^{-1})
$\dot{C}^{f}$ Unit cost of fuel ($·kWh^{-1})
$\dot{C}_{op}$ Annual cost of plant operation ($·year^{-1})
C_p Specific Heat (kJ·(kg·K)$^{-1}$)
$\dot{C}_{total}$ Air constant pressure specific volume (kJ·(kg·K)$^{-1}$)
C_{total} Annual total cost ($·year^{-1})
d_0 Inner diameter of heat exchange tube (m)
d_i Outer diameter of heat exchange tube (m)
$\dot{E}$ Exergy (kW)
F_{of} Surface area (m^2)
F_i Internal surface area (m^2)
F_r Surface area of copper pipe (m^2)
F_f Rib surface area (m^2)
h Specific enthalpy (J·kg^{-1})
U heat transfer coefficient (W·(°C·m^2)$^{-1}$)
i Interest rate (%)
m Mass (ton)
$\dot{m}$ Mass flow rate (kg·s^{-1})
N Equipment service life (year)
P Pressure (Bar)
Q Heat load (kW)
X Mass fraction (%)
r_i Dirt thermal resistance in tube (m^2·°C·W^{-1})
r_o Fouling thermal resistance outside the tube (m^2·°C·W^{-1})
r_P Compression ratio
s Entropy (kJ·(kg·K)$^{-1}$)
t Temperature (°C)
t_0 Ambient temperature (°C)
t_{CL} Cold refrigerated space temperature (°C)
top Annual operation time (hour)
w_y Face velocity (m·s^{-1})
W Power (kW)
Z Cost ($)
$\dot{Z}$ Annual cost ($·year^{-1})

Greek symbols

α_i Heat transfer coefficient inside the tube (W·(°C·m^2)$^{-1}$)
α_o Heat transfer coefficient outside the tube (W·(°C·m^2)$^{-1}$)
ρ_a Air density (kg·m^{-3})
Δ Delta
λ Thermal conductivity of tube wall (W·(m·°C)$^{-1}$)
λ_i Thermal conductivity in tube (W·(m·°C)$^{-1}$)
λ_u Thermal conductivity of frost or water (W·(m·°C)$^{-1}$)
δ Wall thickness (m)
δ_u Thickness of frost or water film (m)
ξ Coefficient of moisture
ξ_u Frost or water film increases the coefficient of air resistance
η_f Rib efficiency
η_{fan} Fan efficiency
η_{Ex} Exergy efficiency
η_s Isentropic efficiency of the compressor
ϕ Maintenance cost factor
μ_{CO_2} Emission conversion factor of electricity from grid

Superscripts

CH Chemical
PH Physical

Subscripts

a Air
Abs Absorber
C Condenser
cas cascade
CE Condensing-evaporator
CA Condenser of high-temperature stage
CC Condenser of low-temperature stage
CL Cold space
CRF Capital recovery factor
D Destruction
E Evaporator
EA Evaporator of high-temperature stage
EC Evaporator of low-temperature stage
Ex Exergy
G Generator
M Middle
R Condensing vapor of high temperature stage
R1 High-pressure vapor of high temperature stage
R2 Low-pressure vapor of high temperature stage
R3 Vapor of low temperature stage
S Strong solution
SW Median solution
W Weak solution
1–23 Status points